Synthesis and Characterization of MgO-QU/GO Nanocomposite and its Antioxidant Study in Zebrafish

Ravichandiran RAGUNATH [1] *****, **Bichandarkoil Jeyaram PRATIMA** [1], **Namasivayam NALINI** [1], **Arunachalam KALIRAJAN** [2], **Jeane Ngala BANDA** [3], **Sharma NEHA** [4], **Arunachalam CHINNATHAMBI** [5], **Sulaiman ALI ALHARBI** [5]

[1] *Department of Biochemistry and Biotechnology, Faculty of Science, Annamalai University, Tamil Nadu, India*
[2] *Department of Chemistry and Biology, School of Natural and Applied Sciences, Mulungushi University, Kabwe 80415, Zambia*
[3] *School of Nursing and Midwifery, Mulungushi University, Kabwe 80415, Zambia*
[4] *Department of Biotechnology, Maharishi Markandeswar, Mullana, Ambala -133207, India*
[5] *Department of Botany and Microbiology, College of Science, King Saud University, PO Box -2455, Riyadh -11451, Saudi Arabia*

The use and manufacture of nanomaterials are expanding, which is concerning for human health. Graphene oxide (GO), magnesium oxide (MgO), and quercetin (QU) have typically had significant growth because of their diverse range of applications in nanomedicine. They are utilised in the treatment of cancer, medication delivery, tissue engineering, healing of wounds, and biosensor. In this work, MgO-QU/GO nanocomposite was synthesized and its antioxidant was tested in a zebrafish model. Further obtained MgO-QU/GO nanocomposite was characterized through UV, XRD, FTIR, and SEM with EDAX analysis. Zebrafish adult seven test groups were used in the experiment with each group containing 10 fish follows fish fed the control, and exposed to MgO-QU/GO nanocomposite concentration 0+0.0+20.0+40.0+80.0+20+0.0+40+0.0+80+0 mg/L. The outcome shows that the toxicity of the utilised nanocomposite was comparatively low after zebrafish were exposed to MgO-QU/GO and recovered. Exploratory MgO-QU/GO treatment to zebrafish significant by decreased the Lipid Peroxidation (LPO) and elevated the antioxidant. These findings imply that nanocomposite at the concentration considered here might be a workable substitute for water recovery as they have no negative effects on the long-term life and welfare of humans and animals.
Keywords: zebrafish,antioxidant,nanocomposite,magnesium oxide,quercetin, graphene oxide.

1. INTRODUCTION

One of the many carbon allotropes is graphite, and it has a lot of potential for use in a variety of fields, including electronics and functional nanocomposite. Due to their hydrophobic nature, both graphite and graphene exhibit peculiar features that may be constrained by their dispensability, particularly when combined with polar polymer matrices. A lot of interest is being paid to graphene-based nanocomposites due to their outstanding physicochemical and biological characteristics. In addition to removing some of their limitations, graphene-nanoparticle composites may enhance the performance of the individual ingredients while maintaining the efficiency of both parts [1]. According to Cornard et al. [2], flavonoids also have a significant impact on the bioavailability of metal ions that are found in small levels in human bodies and lessen the toxicity of several hazardous metals, including Pb (II). Quercetin, a special bioactive flavonoid generated from plant sources, has a catechol-type structure in the B ring, a 2,3,double bond and 4-oxo functional group in the C ring, and a resorcinol-type arrangement of hydroxyl groups in the a ring. In addition, quercetin can act as a defense mechanism against the generation of a few free radicals brought on by

environmental factors like smoking. Cigarette tar is a cause of free radicals that have been established to damage erythrocyte membranes. It was also reported that quercetin and its conjugate metabolites could safeguard erythrocytes from the membranous injury caused by smoking [3]. Over the past two decades, MgO-NPs have been far more popular among researchers than other metal oxide nanoparticles due to their many applications and distinctive features [4 – 6].

Given their importance to human nutrition, fish from contaminated areas may be damaging to people's health. The fact that fish are at the top of the chain of aquatic food sources makes them ideal bioindicators of metal contamination. Metal polluting of the marine environment can be assessed by looking at fish's antioxidant defences and damage due to oxidation, as metals are well-known to produce oxidative stress [7].

Fish feature antioxidant defence systems similar to those in mammals, including the enzyme system and low molecular weight antioxidants, despite the fact that the exact isoforms of enzymes in a variety of fish species have not been thoroughly identified [8]. The primary antioxidant enzymes and significant oxidative stress markers are glutathione peroxidase (GPx), glutathione-s-transferase

*****Corresponding author. Tel.: +91-89734 13182.
E-mail: *g.rani@silsorg.in* (R. Ragunath)

(GST), superoxide dismutase (SOD), catalase (CAT), and glutathione-peroxidase (SOD).

In non-enzymatic antioxidant defence, reduced glutathione (GSH) and oxidised glutathione disulphide (GSSG) are crucial components. In addition to having specific roles in the metabolism and homeostasis of vital metals, metalbinding proteins including ferritin, ceruloplasmin, and metallothioneins (MTs) also play a part in the detoxification of harmful metals [9].

The choice of *Danio rerio* for this investigation was made as it is a standardised organism (OECD 1992) that is frequently utilised in scientific studies due to particular traits like small size, quick growth, minimal cost, significant resemblance to the human genome, simple maintenance under laboratory circumstances [10, 11]. The biochemical, molecular, and behavioural reactions to various NPs have been considered when evaluating the toxicity of this species [11 – 15]. Even though there has been much research on the toxicity of MgO-QU/GO to aquatic creatures, there have only been a few that have looked at how well they can recover in the post-exposure phase when there is no nanocomposite present.

Exposure to nanoparticles may cause metabolic imbalances that last even after the stressor is removed, having serious negative effects on both individuals and societies. Evaluation of recovery is crucial, especially for aquatic biota protection programmes.

2. EXPERIMENTAL

2.1. Synthesis and characterization of MgO-QU/GO nanocomposite

GO was created using a modified version of Hummer's technique from natural graphite powder, with H_2SO_4, $NaNO_3$, and H_2O_2 (30 %) as the starting materials (GO). To prepare the synthetic GO for usage, it was dispersed onto separate sheets in distilled water at a concentration of 0.8 g/mL using an ultra sonicator. The preparation of MgO-QU/GO nanocomposite was carried out as follows (Fig. 1).
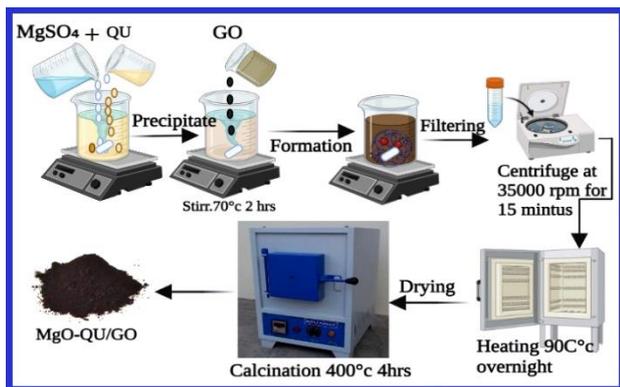
Fig. 1. Synthesis of MgO-QU/GO nanocomposite

In the experiment, 1 g MgSO4 dissolved in 50 ml water was added to 1g quercetin dissolved in 40 ml water. To this 0.8 g GO was added and dispersed using an ultrasonicator for 15 min [13]. The mixture was produced after the solution was agitated for 2 hours at 70 °C and dried for 12 hours in a hot air oven at 90 °C. The brown black dispersion product was centrifuged and washed twice with distilled water and

dispersed in water. The powder was taken in a silica crucible and placed in a muffle furnace at 400 ºC for 2 h, for characterization and future use [15]. The synthesized MgO-QU/GO nanocomposite was characterized using UV-Vis absorption spectroscopy, FT-IR spectroscopy, x-ray diffraction spectrometry and scanning electron microscopy (SEM), energy dispersive x-ray (EDS) analysis.

2.2. Zebrafish treatment, exposure and sample preparation

A neighbourhood fish market in Kolathur, Chennai, Tamil Nadu, provided 70 zebrafish (*Danio rerio*) weighing 1.9302 g. Fish were fed commercial meals three times a day during their one-week acclimatisation period prior to the trial. The water temperature was maintained at 26.0±1.0°C, and the 12L: 12D photoperiod was upheld. The physiochemical parameters of the water were measured daily. Seven test groups were used in the experiment with each group containing 10 fish (Table 1).

Table 1. Protocol for zebrafish treatment.

No.	Test groups	Treatment methods
1	Group 1	0+0 Fish fed the control diet
2	Group 2	0+20 Fish fed the control diet and exposed to MgO-QU/GO nanocomposite (20 mg/L) for 7 days
3	Group 3	0+40, Fish fed the control diet and exposed to MgO-QU/GO nanocomposite (40 mg/L) for 7 days
4	Group 4	0+80 Fish fed the control diet and exposed to MgO-QU/GO nanocomposite (80 mg/L) for 7 days
5	Group 5	0+20+0 Fish fed the control diet and exposed to MgO-QU/GO nanocomposite (20 mg/L) water for the first 5 days, followed by fresh water for 2days
6	Group 6	0+40+0 Fish fed the control diet and exposed to MgO-QU/GO nanocomposite (40 mg/L) water for the first 5 days, followed by fresh water for 2days
7	Group 7	0+80+0 Fish fed the control diet and exposed to MgO-QU/GO nanocomposite (80 mg/L) water for the first 5 days, followed by fresh water for 2days

In 3L aquariums, fish were randomly distributed. Each group of fish under investigation was exposed to MgO-QU/GO nanocomposite. The fish in groups 2, 3, and 4 were maintained in a 3L tank and every day for 7 days each liter of water was replaced with MgO-QU/GO nanocomposite containing water. The fish in group 5, 6, and 7 were maintained in MgO-QU/GO for 5 days. After 5 days of nanocomposite exposure, the fish were transferred to clean water and maintained for 2 days as a recovery period. For 7 days, fish were fed twice a day; at 10:00 a.m. and 3:00 p.m.

Sampling was done 7 days following the exposure of nanoparticles.

Each group slaughtered 70 fish, and liver tissue samples were taken from those animals. The tissue was promptly homogenised (10 volume) in a 0.9 % cold saline solution. After centrifuging the homogenate at 2500 g for 15 min at 4 °C, the supernatant was diluted to different quantities, kept at 80 °C, and then subjected to biochemical analysis.

2.3. Oxidative stress index assay

The method used by Kakkar et al. [16] was used to measure the activity of superoxide dismutase (SOD, E.C.1.15.1.1) for the assay relies on inhibiting the formation of NADH-phenazine methosulphate nitroblue tetrazolium formazan. The process starts with the introduction of NADH and incubation for 90 seconds. Glacial acetic acid is subsequently introduced to terminate the reaction. After the reaction concludes, the resulting color is transferred to the n-butanol layer for extraction, followed by measuring the absorbance at 560 nm using a spectrophotometer, while Sinha et al. [17] used it to measure catalase (CAT, E.C.1.11.1.6), when hydrogen peroxide (H_2O_2) is present, heating dichromate in acetic acid causes it to transform into perchromic acid, and subsequently into chromic acetate. The enzyme catalase (CAT) is then permitted to decompose H_2O_2 for different durations. The reaction is halted at various time points by adding a mixture of dichromate-acetic acid, and the remaining H_2O_2, now as chromic acetate, is quantified using a spectrophotometer set at 620 nm. Devasagayam and Tarachand et al. [18] used it to measure glutathione peroxide (Gpx), When reduced glutathione (GSH) is present, a specified quantity of enzyme preparation is allowed to react with H_2O_2 for a predetermined duration. The consumption of GSH is then measured using a spectrophotometer at 420 nm.

3. RESULTS

3.1. Characterization of MgO-QU/GO nanocomposite

3.1.1. UV-Visspectroscopy

The optical studies of the synthesized MgO, QU, GO and MgO-QU/GO samples are shown in Fig. 2. The UV-Vis spectra of MgO, QU, GO were found to be at 282, 250 and 216 nm respectively. In the MgO-QU/GO nanocomposite, a shift of the spectrum to higher wavelengths of 330 nm and 285 nm, and 240 nm region indicates the formation of nanocomposite. The change in the peak position with slight variations observed in the intensity of peaks could be attributed to the size effect of quercetin (QU) added to the nanocomposite.

3.1.2. X-ray diffraction analysis (XRD)

The powder XRD patterns of bare GO, MgO, QU and MgO-QU/GO nanocomposite sample are shown in Fig. 3. The XRD pattern of GO exhibited a peak at 2θ values 11.36 which corresponds to the plane (002). In bare MgO, QU, GO and MgO-QU/GO nanocomposite exhibited the diffraction peaks at 2θ values of 12.8, 18.7, 32.1, 37.9, 50.4, 58.6, and 61.0 to the lattice planes (0 0 2), (1 0 1), (1 1 1), (2 0 0), (2 2 0), (2 2 1), (3 1 1), and (2 2 2) of MgO-QU/GO nanocomposite. The typical peaks agreed with the hexagonal plane of MgO (JCPDS no 76-1363). The changes in the peak position of bare GO, MgO-QU/GO nanocomposite the coexistence of (0 0 2) plane diffraction peak (2θ = 12.8) from carbon structure and changes in the peak position of characteristic peaks indicated that the MgO-QU/GO nanocomposite was assorted without phase transformation.
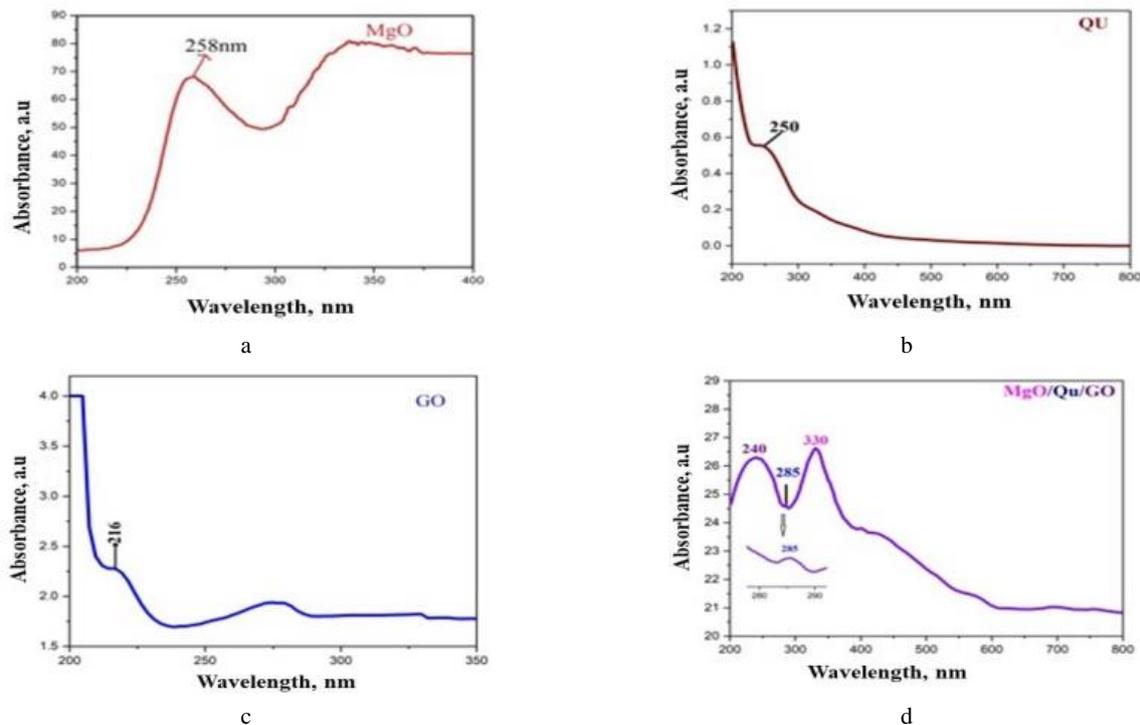
Fig. 2. UV-Vis spectra haracterization: a – MgO; b – QU; c – GO; d – MgO-QU/GO.

Moreover, this peak intensity was shifted when compared to bare GO, MgO, QU. Crystalline size of the synthesized nanocomposite was calculated from the Debye–Scherrer equation $D = K\lambda/\beta\cos\theta$, where D = crystal size, β = full width half maximum of the peak, λ = X-ray wavelength (1.54 Å), K = shape factor which is always close to unity (0.94). The particle size was found to be 12.4, 54.4, 23.5 and 53.3 nm for GO, MgO, QU and MgO-QU/GO samples respectively.
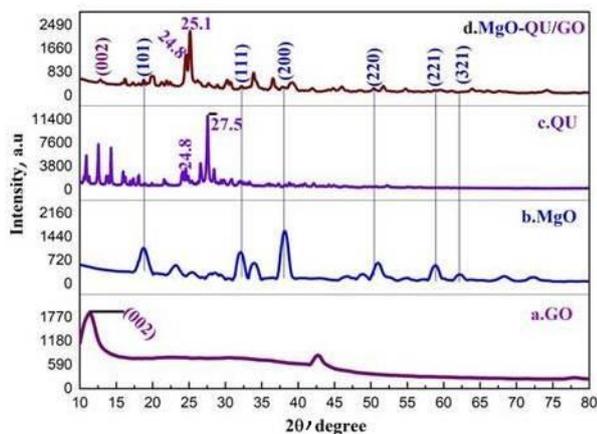
Fig. 3. X-ray diffraction patterns: a – GO; b – MgO; c – QU; d – MgO-QU/GO

3.1.3. Fourier transform infrared spectroscopy analysis (FT-IR)

The MgO-QU/GO nanocomposite's FT-IR spectra are displayed in Fig. 4. The hydroxyl, carboxylic, and aromatic groups of quercetin are attributed to the distinctive vibrations in the range of 900 – 1600 cm^{-1} that were seen in the spectra of bare quercetin (Fig. 4 c). Stretching of the -OH and aromatic carbonyl groups are responsible for the distinctive vibrations at 3409 cm^{-1}, 1384 cm^{-1}, and 1664 cm^{-1}, respectively. The quercetin's C-H stretching vibration is represented by the bands at 2927 cm^{-1} and 2852 cm^{-1}, respectively. Additionally, the strong vibrations of C=O and C–H were seen at 1014 cm^{-1} and 941 cm^{-1}, respectively. The bare MgO peak (Fig. 4 b) corresponds to the distinctive vibrations at 669 cm^{-1} and 455 cm^{-1} in the MgO-QU/GO nanocomposite spectrum seen in Fig. 4 d. Additionally, significant band shifts in the MgO-quercetin nanocomposite's signature vibration bands were found. Quercetin and MgO-QU/GO nanocomposite both showed the C–H stretching vibration at 2927 cm^{-1} and 2852 cm^{-1}, respectively, without any changes in the intensity of the vibration peaks, demonstrating the retention of quercetin structure even after their attachment to MgO nanoparticles. It is interesting to notice that the peak intensity of the –OH group's stretching vibration at 1384 cm^{-1} was displaced in the MgO-QU/GO nanocomposite, which may indicate that MgO is the primary material with which quercetin's –OH group interacts during the production of the nanocomposite. Additionally, the involvement of the –OH group resulted in a shift in the C–O band's stretching vibration from 1168 cm^{-1} to 1142 cm^{-1} [19]. Due to the oxidation of the –OH group, which led to the creation of intermolecular hydrogen bonds and a shift in the C=O vibration band from 1664 cm^{-1} to 1608 cm^{-1}, it is confirmed that –OH groups are involved in

the production of the MgO-QU/GO nanocomposite [19, 20].

The FT-IR spectra of GO, MgO, QU, and MgO-QU/GO nanocomposite are displayed in Fig. 4 a – d. In the MgO-QU/GO nanocomposite, it is clear from the spectrum that GO exhibits the typical vibrations at 2971 cm^{-1}, where C–O stretching was shifted to 2972 cm^{-1}, C–H stretching vibrations, and 1386 cm^{-1} to C–O deformation was shifted to 1384 cm^{-1} to OH groups stretching vibration (Fig. 4 d). However, no significant vibrational alterations were seen, demonstrating that the GO structure was retained even after being attached to the MgO-QU/GO nanocomposite.
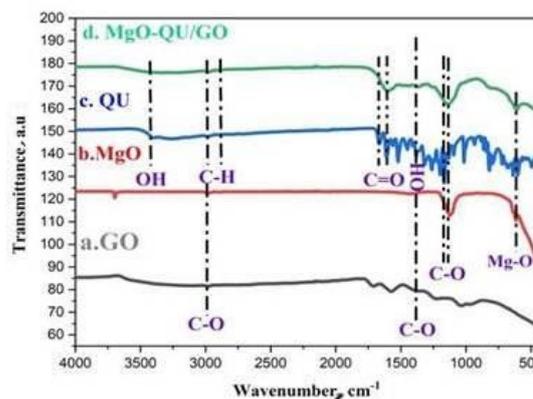
Fig. 4. FT-IR spectra: a – GO; b – MgO; c – QU; d – MgO-QU/GO

3.1.4. Scanning electron microscopy analysis (SEM) and Energy-dispersive x-ray spectroscopy analysis (EDS)

The structure and morphology of MgO-QU/GO nanocomposite were analysed by scanning electron microscopy. Here the morphologies of homogenous MgO, QU, GO and heterogenous MgO-QU/GO nanocomposite were compared. Fig. 5 a shows the cubic shaped morphology of MgO NPs. Fig. 5 b, represents the rod-like structure of quercetin, the surface of which appears to be smooth.
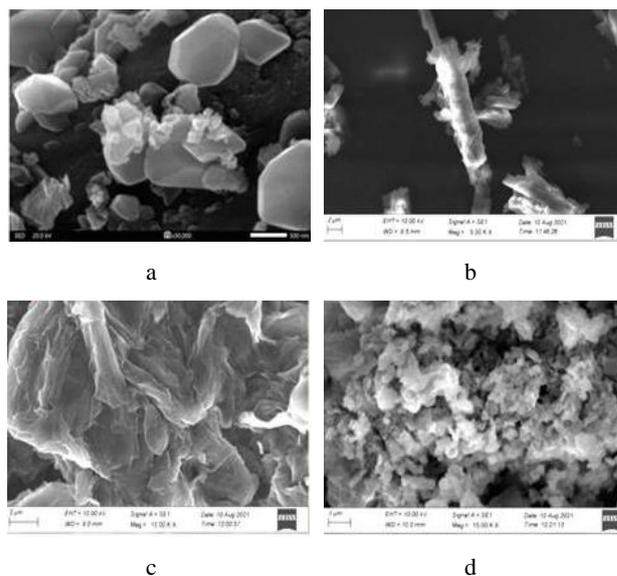
Fig. 5. Scanning electron microscopy analysis: a – MgO; b – QU; c – GO; d – MgO-QU/GO

Fig. 5 c shows a thin layer with wrinkles and folds exhibiting GO. Fig. 5 d shows the different magnifications of MgO-QU/GO nanocomposite at 1 µm, 2 µm, 200 µm, respectively. The rod-like granules and cubic shaped MgO-QU were uniformly decorated on the surface of the GO nanosheets, which was evident from the SEM micrographs. The produced nanocomposite's elemental composition was verified using the energy dispersive X-ray spectroscopy (EDS). Fig. 6 MgO-QU/GO nanocomposite was analysed by using EDS, which confirmed the presence of C and O, Mg in the MgO-QU/GO nanocomposite respectively. EDS analysis of MgO-QU/GO, showed the peak (C mass % 8.61 ± 0.14, atom % 12.52 ± 0.21), (O mass % 58.40 ± 0.30, atom % 63.77 ± 0.33), (Mg mass % 32.99 ± 0.22, atom % 23.70 ± 0.16) confirming the presence of C, Mg, O in the prepared nanocomposite.
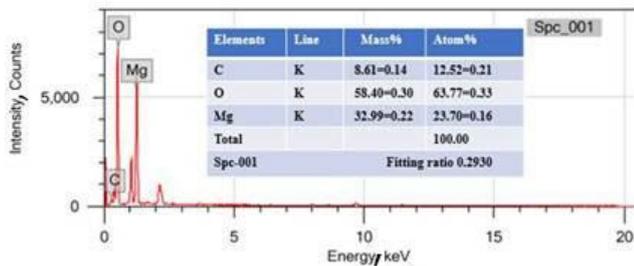
Fig. 6. EDAX measurement of the nanocomposite MgO-QU/GO

3.2. Zebrafish exposure to MgO-QU/GO and recovery

The fish group 0+40's liver SOD activity was shown to have significantly increased. The liver CAT activity was also increased in the 0+40 group when compared to the control 0+0 groups proving that the nanocomposite showed effective antioxidant activity. The activity of GPx in the liver was decreased in the 0+40 MgO-QU/GO treated fish group. There was an increase in LPO in 0+80+0 fish group. These outcomes were seen five days after being exposed to MgO-QU/GO (Fig. 7 a – d). Following two days of recovery without MgO-QU/GO, the 0+40 fish group's SOD activity remained elevated. After the recovery period, the CAT's activity remained unaltered. The GPx activity was increased in 0+20 and 0+40 fish even after the recovery period (Fig. 7 a – d).

4. DISCUSSION

Products made from carbon nanomaterials have seen an increase in commercial use recently, and this trend is expected to continue [21]. Freshwater environments are more likely to receive releases of GO at pertinent concentrations. From an ecotoxicological point of view, GO can have toxic effects in these conditions on aquatic animals, which could be substantial, particularly in terms of protecting the aquatic food chain's balance. Gill cell antioxidant enzyme activity was altered in adult zebrafish exposed to GO over 48 hours, showing the impacts of oxidative stress. Because the organism's gills are its first line of defence against pollutants in the aquatic environment, when conditions are bad, its defences are promptly engaged. According to Chen et al. [13], normal metabolism in the body shows stability between ROS production and ROS removal through antioxidant enzymatic activities. However, in unfavourable circumstances, this system may become unstable and lead to oxidative stress, which can seriously harm tissues, particularly membranes.
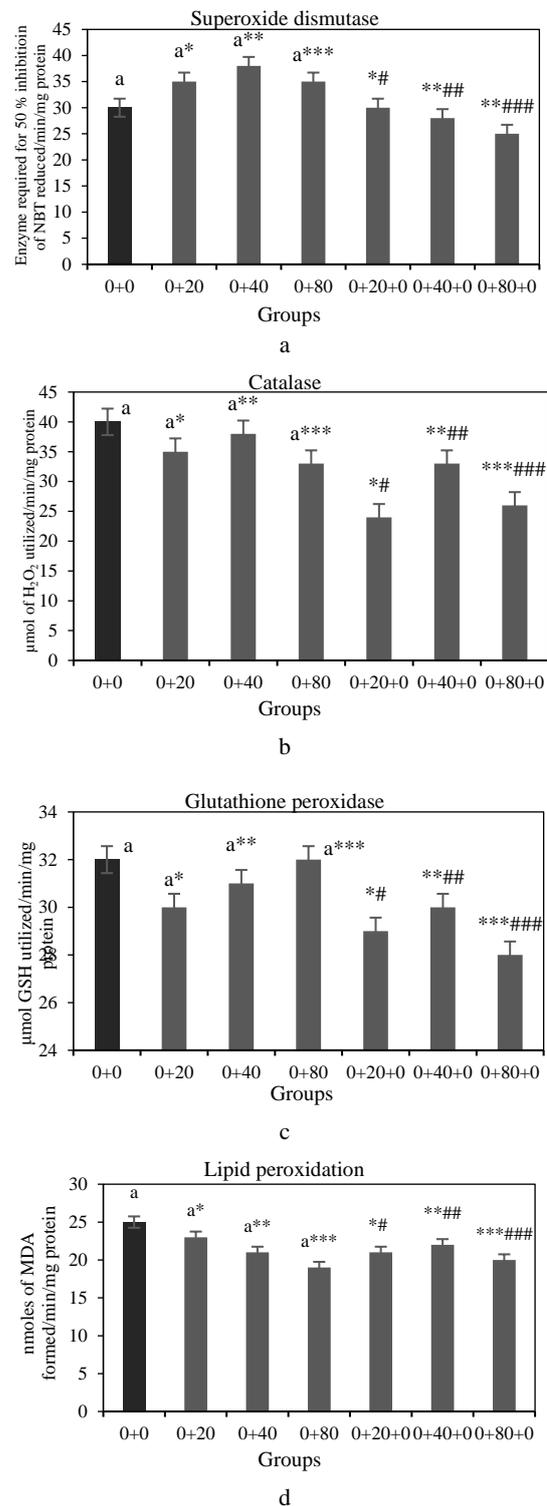
Fig. 7. Graphs depicting the amount: a – superoxide dismutase (SOD); b – catalase (CAT); c – glutathione peroxidase (GPx); d – lipid peroxidation (LPO) activity in the control; MgO-QU/GO exposure and recovery groups. In data, the mean and standard error of the mean are used. Significant differences between the groups are denoted by different letters (p 0.05)

After 5 days of exposure to MgO-QU/GO at a concentration of 40 mg/L (0+40), SOD and CAT activities were markedly increased in our study. Furthermore, GPx activity was decreased during this period, and LPO concentrations increased in the 80 mg/L (0+80).

SOD is the first antioxidant defence mechanism to be activated in the presence of hazardous substances, such as NPs [13, 22]. This enzyme protects tissues from superoxide anion radicals by catalysing the production of H_2O_2, which is then detoxified by CAT and GPx enzymes [23]. The SOD-CAT pair's activation throughout a 48-hour exposure shows that CAT cleared the H_2O_2 generated by SOD activity. However, it's possible that this clearance wasn't carried out efficiently, which led to GPx's reduced activity because of scavenging the extra free radicals. In this context, it has been demonstrated that peroxidases can be inactivated by superoxide radicals generated by detoxifying activities [25]. We suggest that exposure to MgO-QU/GO (0+40) can sufficiently activate antioxidant enzymes like SOD and CAT to prevent ROS and LPO chain production.

Other investigators have found increased SOD and CAT activities as well as oxidative stress in response to carbon nanomaterials [12, 13, 26]. A 14-day exposure to MgO-QU/GO resulted in increased SOD, CAT, and TBARS content, as well as a decrease in glutathione levels in the liver [13]. Previous studies have detected increased ROS formation following MgO-QU/GO exposure, as well as histological alterations in the adult zebrafish gills, liver, and digestive tract tissues [12]. Nanocomposite interactions with cell membranes, can trigger antioxidant defense when zebrafish are subjected to harmful conditions in 0+40 fish which showed enhanced SOD and CAT activity. Fernandes et al. [26] discovered that graphene concentration at 50 mg/L was toxic to gill cells, as evidenced by increased lipid peroxidation levels and decreased antioxidant levels. A similar relationship exists between elevated oxidative stress and cellular damage and changed quantities of antioxidant enzymes and proteins. These consequences are significant because they may alter the aquatic food web and threaten the existence of other fish species.

After two days of zebrafish exposure to clean water without MgO-QU/GO, SOD activity increased but CAT and the GPx activity remained unaffected. The Lipid Peroxidation (LPO) activity was reduced. These findings suggest that an increase in SOD activity activated the initial antioxidant defense mechanism, giving substrate for CAT, which thereafter recovered to control levels. However, the reduced GPx activity in the fish group exposed to 0+80 raised two hypotheses: one is that excess of H2O2 produced, because of the unchanged CAT activity, decreased GPx activity; record, the increased SOD activity was able to scavenge the oxyradicals, and CAT and GPx were no longer required. It's interesting to note that even when GPx activity was reduced, there was no LPO. This is probably because protective mechanisms in zebrafish gill tissues closely control the amount of LPO thereby stopping its propagation or reducing its content. The lower LPO discovered during recovery lends credence to the assertion that SOD activity is sufficient to avert oxidative damage in zebrafish gills. In this regard, Chupani et al. [27] found that exposure to zinc oxide nanoparticles resulted in a decrease in Lipid Peroxidation in the liver of a common carp. In the absence of MgO-QU/GO,

it is plausible that the adaptive reactions occurred throughout the recovery phase. These adaptive reactions were enough to prevent LPO, but antioxidant enzyme activity was restored to near-normal levels, suggesting that the nanocomposite may be successful at boosting antioxidant levels and hence useful for therapeutic purposes.

According to Lushchak et al. [23], depending on the degree of oxidative stress, physiologic condition, severity, and kind of stress, organisms can display adaptive responses. We believe that MgO-QU/GO exposure increased antioxidant defenses in zebrafish; nevertheless, when the organism was allowed to recuperate in clean water, there were no harmful consequences following the exposure. In other investigations, antioxidant defenses were boosted in the first hours of exposure, but returning to the previous circumstances was enough to attenuate the harmful effects, including LPO formation [24, 28]. Antioxidant defenses are often coordinated to provide protection against oxidative stress [28]. However, adequate conditions must be supplied for physiological parameters to be restored. Organisms are unable to recover when stress events last for an extended period or when stress levels are high. Antioxidant responses are extremely sensitive to cause-and-effect relationships. These reactions emphasize the importance of evaluating different endpoints, such as histological, molecular, and ROS production characteristics [26].

5. CONCLUSIONS

In summary, our thorough examination of the synthesized MgO, QU, GO, and MgO-QU/GO nanocomposite has uncovered noteworthy alterations in optical, structural, and chemical characteristics. The UV-Vis spectrum has pointed to a discernible shift in the MgO-QU/GO nanocomposite, implying its successful formation without undergoing any phase transformation. This shift is likely influenced by the size effect of quercetin. The X-ray diffraction analysis has corroborated the presence of a hexagonal plane of MgO in the nanocomposite, with calculated crystalline sizes displaying variations among the samples.

Insights into the interactions between MgO, QU, GO, and the nanocomposite were gained through Fourier Transform Infrared Spectroscopy (FT-IR) analysis. The distinctive vibrations and peak shifts observed in characteristic spectra imply the preservation of quercetin structure and the participation of -OH groups in the production of the MgO-QU/GO nanocomposite.

Morphological assessments, as depicted by Scanning Electron Microscopy (SEM) and Energy-dispersive X-ray Spectroscopy (EDS), visually showcased the structures of individual components and the uniform distribution of MgO-QU on GO nanosheets. EDS further verified the presence of C, Mg, and O in the nanocomposite.

The biological assessment involving zebrafish exposed to MgO-QU/GO unveiled substantial alterations in antioxidant enzyme activities and lipid peroxidation levels in the liver. The nanocomposite demonstrated effective antioxidant activity, evident from heightened superoxide dismutase (SOD) and catalase (CAT) activities, along with diminished glutathione peroxidase (GPx) activity. Notably,

the recovery phase exhibited a persistent elevation in SOD activity, suggesting enduring antioxidant effects.

Our study emphasizes the potential of the MgO-QU/GO nanocomposite as an antioxidant with potential therapeutic applications. However, to ensure the safe utilization of such nanocomposites in practical scenarios, further investigations into potential toxicity and long-term effects are imperative. These findings significantly contribute to the understanding of nanocomposite interactions with biological systems, emphasizing the need to assess various endpoints for a comprehensive evaluation.

REFERENCES

1. **Gurunathan, S., Kang, M.H., Jeyaraj, M., Kim, J.H.** Differential Cytotoxicity of Different Sizes of Graphene Oxide Nanoparticles in Leydig (TM3) and Sertoli (TM4) Cells *Nanomaterials* 9 (2) 2019: pp. 139. https://doi.org/10.3390/nano9020139

2. **Cornard, J.P., Dangleterre, L., Lapouge, C.** Computational and Spectroscopic Characterization of the Molecular and Electronic Structure of the Pb (II)− Quercetin Complex *The Journal of Physical Chemistry A* 109 (44) 2005: pp. 10044 – 10051. https://doi.org/10.1021/jp053506i

3. **Begum, A.N., Terao, J.** Protective Effect of Quercetin Against Cigarette Tar Extract-Induced Impairment of Erythrocyte Deformability *The Journal of Nutritional Biochemistry* 13 (5) 2002: pp. 265 – 272. https://doi.org/10.1016/s0955-2863(01)00219-4

4. **Din, M.I., Najeeb, J., Ahmad, G.** Recent Advancements in the Architecting Schemes of Zinc Oxide-Based Photocatalytic Assemblies *Separation & Purification Reviews* 47 (4) 2018: pp. 267 – 287. https://doi.org/10.1080/15422119.2017.1383918

5. **Jeevanandam, J., San Chan, Y., Danquah, M.K.** Evaluating the Antibacterial Activity of MgO Nanoparticles Synthesized from Aqueous Leaf Extract *Med One* 4 (3) 2019: pp. e190011. https://doi.org/10.20900/mo.20190011

6. **Rani, P., Kaur, G., Rao, K.V., Singh, J., Rawat, M.** Impact of Green Synthesized Metal Oxide Nanoparticles on Seed Germination and Seedling Growth of Vigna radiata (Mung Bean) and Cajanus cajan (Red Gram) *Journal of Inorganic and Organometallic Polymers and Materials* 30 2020: pp. 4053 – 4062. https://doi.org/10.1007/s10904-020-01551-4

7. **Livingstone, D.R.** Oxidative Stress in Aquatic Organisms in Relation to Pollution and Aquaculture *Revue de Médecine Vétérinaire* 154 (6) 2003: pp. 427 – 430.

8. **Di Giulio, R.T., Hinton, D.E.** The Toxicology of Fishes *CRC Press* 2008: pp. 1096. https://doi.org/10.1201/9780203647295

9. **Kelly, K.A., Havrilla, C.M., Brady, T.C., Abramo, K. H., Levin, E.D.** Oxidative Stress in Toxicology: Established Mammalian and Emerging Piscine Model Systems *Environmental health perspectives* 106 (7) 1998: pp. 375 – 384. https://doi.org/10.1289/ehp.98106375

10. **Barbazuk, W.B., Korf, I., Kadavi, C., Heyen, J., Tate, S., Wun, E., Johnson, S.L.** The Syntenic Relationship of the Zebrafish and Human Genomes *Genome Research* 10 (9) 2000: pp. 1351 – 1358. https://doi.org/10.1101/gr.144700

11. **Souza, J.P., Baretta, J.F., Santos, F., Paino, I.M., Zucolotto, V.** Toxicological Effects of Graphene Oxide on Adult Zebrafish (Danio rerio) *Aquatic Toxicology* 186 2017: pp. 11 – 18. https://doi.org/10.1016/j.aquatox.2017.02.017

12. **Chen, M., Yin, J., Liang, Y., Yuan, S., Wang, F., Song, M., Wang, H.** Oxidative Stress and Immunotoxicity induced by Graphene Oxide in Zebrafish *Aquatic Toxicology* 174 2016: pp. 54 – 60. https://doi.org/10.1016/j.aquatox.2016.02.015

13. **Chen, Y., Hu, X., Sun, J., Zhou, Q.** Specific Nanotoxicity of Graphene Oxide During Zebrafish Embryogenesis *Nanotoxicology* 10 (1) 2016: pp. 42 – 52. https://doi.org/10.3109/17435390.2015.1005032

14. **Zhang, P., Selck, H., Tangaa, S.R., Pang, C., Zhao, B.** Bioaccumulation and Effects of Sediment-Associated Gold- and Graphene Oxide Nanoparticles on Tubifex Tubifex *Journal of Environmental Sciences* 51 2017: pp. 138 – 145. https://doi.org/10.1016/j.jes.2016.08.015

15. **Zhang, X., Zhou, Q., Zou, W., Hu, X.** Molecular Mechanisms of Developmental Toxicity Induced by Graphene Oxide at Predicted Environmental Concentrations *Environmental Science &Technology* 51 (14) 2017: pp. 7861 – 7871. https://doi.org/10.1021/acs.est.7b01922

16. **Kakkar, P., Das, B., Viswanathan, P.N.** A Modified Spectrophotometric Assay of Superoxide Dismutase *Indian Journal of Biochemistry and Biophysics* 21 (2) 1984: pp. 130 – 132.

17. **Sinha, A.K.** Colorimetric Assay of Catalase *Analytical biochemistry* 47 (2) 1972: pp. 389 – 394. https://doi.org/10.1016/0003-2697(72)90132-7

18. **Devasagayam, T.P., Tarachand, U.** Decreased Lipid Peroxidation in the Rat Kidney During Gestation *Biochemical and Biophysical Research Communications* 145 (1) 1987: pp. 134 – 138. https://doi.org/10.1016/0006-291x(87)91297-6

19. **Sathishkumar, P., Li, Z., Huang, B., Guo, X., Zhan, Q., Wang, C., Gu, F.L.** Understanding the Surface Functionalization of Myricetin-Mediated Gold Nanoparticles: Experimental and Theoretical Approaches *Applied Surface Science* 493 2019: pp. 634 – 644. https://doi.org/10.1016/j.apsusc.2019.07.010

20. **Guo, Q., Guo, Q., Yuan, J., Zeng, J.** Biosynthesis of Gold Nanoparticles Using a Kind of Flavonol: Dihydromyricetin *Colloids and Surfaces A: Physicochemical and Engineering Aspects* 441 2014: pp. 127 – 132. https://doi.org/10.1016/j.colsurfa.2013.08.067

21. **Zhao, J., Wang, Z., White, J.C., Xing, B.** Graphene in the Aquatic Environment: Adsorption, Dispersion, Toxicity and Transformation *Environmental Science &Technology* 48 (17) 2014: 9995 – 10009. https://doi.org/10.1021/es5022679

22. **Lushchak, V.I.** Environmentally Induced Oxidative Stress in Aquatic Animals *Aquatic Toxicology* 101 (1) 2011: pp. 13 – 30. https://doi.org/10.1016/j.aquatox.2010.10.006

23. **Lushchak, V.I.** Adaptive Response to Oxidative Stress: Bacteria, Fungi, Plants and Animals *Comparative*

Biochemistry and Physiology Part C: Toxicology & Pharmacology 153 (2) 2011: pp. 175 – 190.
https://doi.org/10.1016/j.cbpc.2010.10.004

24. **Lushchak, V.I., Bagnyukova, T.V., Lushchak, V., Storey, J.M., Storey, K.B.** Hypoxia and Recovery Perturb Free Radical Processes and Antioxidant Potential in Common Carp (Cyprinus Carpio) Tissues *The International Journal of Biochemistry & Cell Biology* 37 (6) 2005: pp. 1319 – 1330.
https://doi.org/10.1016/j.biocel.2005.01.006

25. **Odajima, T., Yamazaki, I.** Myeloperoxidase of the Leukocyte of Normal Blood iii. The Reaction of Ferric Myeloperoxidase with Superoxide Anion *Biochimica et Biophysica Acta (BBA)-Enzymology* 284 (2) 1972: pp. 355 – 359.
https://doi.org/10.1016/0005-2744(70)90083-5

26. **Fernandes, A.S., Mazzei, J.L., Evangelista, H., Marques, M.R.C., Ferraz, E.R.A., Felzenszwalb, I.** Protection Against Uv-Induced Oxidative Stress and DNA Damage by Amazon Moss Extracts *Journal of Photochemistry and Photobiology B: Biology* 183 2018: pp. 331 – 341.
https://doi.org/10.1016/j.jphotobiol.2018.04.038

27. **Chupani, L., Niksirat, H., Velíšek, J., Stará, A., Hradilová, Š., Kolařík, J., Zusková, E.** Chronic Dietary Toxicity of Zinc Oxide Nanoparticles in Common Carp (cyprinus carpio l.): Tissue Accumulation and Physiological Responses *Ecotoxicology and Environmental Safety* 147 2018: pp. 110 – 116.
https://doi.org/10.1016/j.ecoenv.2017.08.024

28. **Bagnyukova, T.V., Chahrak, O.I., Lushchak, V.I.** Coordinated Response of Goldfish Antioxidant Defenses to Environmental Stress *Aquatic Toxicology* 78 (4) 2006: pp. 325 – 331.
https://doi.org/10.1016/j.aquatox.2006.04.005